

SCALE EFFECT IN DESIGN OF THE PRE-STRESSED MICRO-DIES FOR MICROFORMING

WOJCIECH PRESZ

*Institute of Manufacturing Technologies, Warsaw University of Technology – Narbutta 85,
02-524 Warsaw, Poland*

Corresponding author: w.presz@wip.pw.edu.pl

Abstract

In dies for cold extrusion permissible internal pressure may be increased by the use of one or two shrink rings. Such design creates tensile stresses in the ring and compressive stresses in the insert. The design essentially boils down to define the diametrical interference of the fit to be attained during the assembly. Interference determines the properties of the die and must be carefully selected. There are basically two methods of design: based on Lamé's solution and FEM. None of these two methods include roughness of interface surfaces of the die and shrink ring. The pre-stressed micro-die shows that interface roughness can't be skipped and the "classical" design of diameter interference must be corrected. The novel method of determination of the correction value is introduced: TheSemi-Physical Modelling of models representing Interface Roughness, SPMIR method. In this method a set of FEM modelling of models created on the base of Abbot-Firestone curves, determined from the roughness profile, lead to determination of Contact Surface Stiffness Curve of interface surface and further to interference correction. Relative correction of the die diameter interference increases along with the diameter decrease that might be recognized as a *pre-stressed micro-die assembling scale effect*. For the worked example, the relative interference correction is hyperbolically increasing with decreasing the interface diameter decrease, exceeding 10 % for diameter about 8 mm, 25 % for 3 mm and almost 40% for 2 mm. The proposed method is than recommended for the design of pre-stressed micro dies with interface diameter lower than 8 mm.

Key words: Microforming, Pre-stressed Micro-die, scale effect

1. INTRODUCTION

Cold extrusion of metals and alloys provides a good surface quality and dimensional accuracy comparable even to these obtained by grinding (Lange, 1985). This technology is particularly useful for manufacturing of micro-parts (Presz & Rosochowski, 2006; Geiger, 2001). For billets of materials with relative high plastic resistance the main process limiting factor appears to be a tools strength. In case of dies, it is reduced to the maximal inside pressure that the die can endure. This pressure might be calculated on the base of classical Lamé's theory treating a die as a thick cylinder loaded with internal pressure. The maximum inside pressure is of 1000 MPa for tool materials which are properly chosen

after right hit treatment. It may be increased by the use of one or two shrink rings (Sieber, 1971; Presz, 2009). After the assembling the insert is crimped by the ring/rings. It creates tensile stresses in the ring and compressive stresses in the die that increases permissible pressure inside its cavity. The design essentially boils down to define the radial/diametrical interference fit to be attained during the assembly. In design of such a die one should be extremely careful. Too small interference do not provide enough pre-stressing to protect the die from cracking because of circumferential tension during the load. On the other hand, too big interference might cause crack of the ring during the assembling.

2. PRE-STRESSED MICRO-DIE

Two-piece cylindrical pre-stressed micro-die with inside diameter $d=1$ mm and interface diameter $d_{int} = 2.8$ mm was designed for investigation of micro forming extrusion processes. Vancrone 40 and Orvar Supreme steels were chosen for die and ring. Composition and properties of these materials are shown in table 1.

It was decided to use conical assembling as pre-stressing method. Basic dimensions and assembling procedure are shown in figure 1. The design means finding a right value of interference between die and shrink-ring. In practice interference is controlled by the h_N – distance between the die bottom and the ring bottom before assembling, (1), (2), figure1b. For presented micro-die:

Table 1. Composition and properties of chosen steels

	Material / [%]	C	Cr	Mn	Mo	Si	V	W	N
1	Vancron 40	1.1	4.5	0.4	3.2	0.5	8.5	3.7	1.8
2	Orvar Supreme	0.39	5.2	0.4	1.4	1	0.9	-	-

		Material/Properties	Hardness	Mod. of elasticity	Poisson ratio	Compressive Strength	Tensile stren., Yield
		Unit	[HRC]	[GPa]	[1]	[MPa]	[MPa]
1	Die	Vancron 40	64	236	0.3	2700	-
2	Ring	Orvar Supreme	48	210	0.3	-	1520

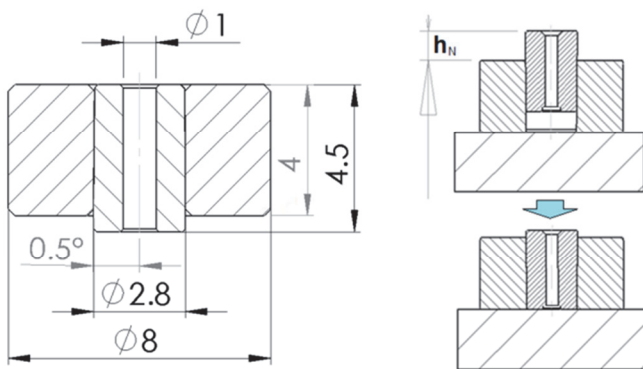


Fig. 1. Basic dimensions of pre-stressed micro-die (left). Assembling procedure (right).

$$h_N = h_{Nr} + 0.5 \text{ [mm]} \tag{1}$$

$$h_{Nr} = \frac{N_r}{\text{tg}0.5^\circ} \text{ [mm]} \tag{2}$$

where: h_{Nr} – axial movement of die during assembling, N_r – radial interference.

Two methods of calculation of interference are basically used: analytical – based on Lamé solution and FEM. In case of die with simple shape both methods give practically the same results that might be seen in figure 2, Marc Mentat 2015.0.0.

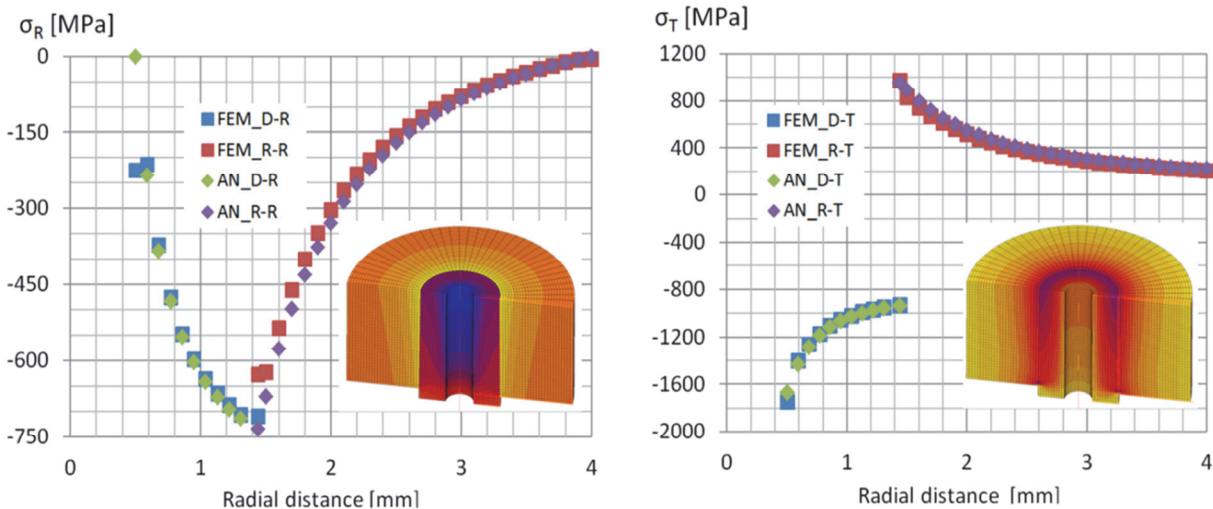


Fig. 2. Distribution of radial and tangential stresses obtained by analytical and FEM methods of analysis.



Diameter interference were obtained by both calculation methods $N_m = 0.02034$ mm, that means radial interference $N_r = 0.01017$ mm. It implicates interface pressure $p = 740$ MPa, figure 2 and assembling high $h_N = 1.665$ mm, (1), (2). Interference seems to be significantly small due to the fact that during assembling the flattening of roughness asperities of interface surfaces either die or ring should be expected, figure 3.

In consequence the reduction of calculated value of interference N_r to real value N_{r-real} occurs according to (3).

$$N_{r-real} = N_r - \Delta N_{r1} - \Delta N_{r2} \quad (3)$$

where: N_r - calculated radial interference, N_{r-real} - real radial interference, ΔN_{r1} - flattening of die asperities, ΔN_{r2} - flattening of ring asperities.

The right design of pre-stressed micro-die must than take interference correction ΔN_r into account because of already mentioned flattening. It leads to the right value of interference N_{r-cor} (4), (5).

$$N_{r-cor} = N_r + \Delta N_r \quad (4)$$

where: $\Delta N_r = \Delta N_{r1} + \Delta N_{r2}$ (5)

3. DETERMINATION OF INTERFERENCE CORRECTION – SPMIR -METHOD

The new method of pre-stressed micro-die design is being introduced. The design is following the scheme shown in figure 4.

The novel part of design is a method which determines the correction value of interference - *SPMIR Method*, Semi-Physical Modelling of models representing Interface Roughness. It is based on FEM modelling of deformation of FEM models of single *representative* asperities of die and ring.

The starting point is the surface profile that leads to Abbot-Firestone curve (Lipa & Tomanickova, 2011) which describes the surface texture. This curve may be found from profile trace by drawing lines parallel to the datum and measuring the fraction of the line which lies within the profile. For the analysed micro-die it can be noticed that the surface profile was taken on its axis direction by Talysurf PGI 830 profilometer, figure 5a.

A representative asperity was than determined, figure 5c according to the Abbot-Firestone curve and standard roughness parameters R_S and R_t , figure 5b. The most important for understanding the idea is to

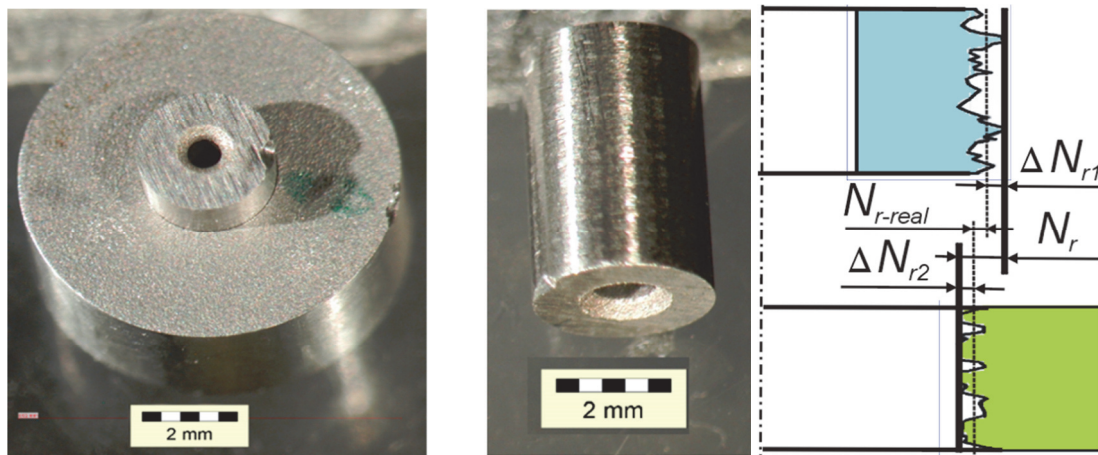


Fig. 3. Micro-die before assembling (left). Die insert (middle). Interference proposed parameters (right).

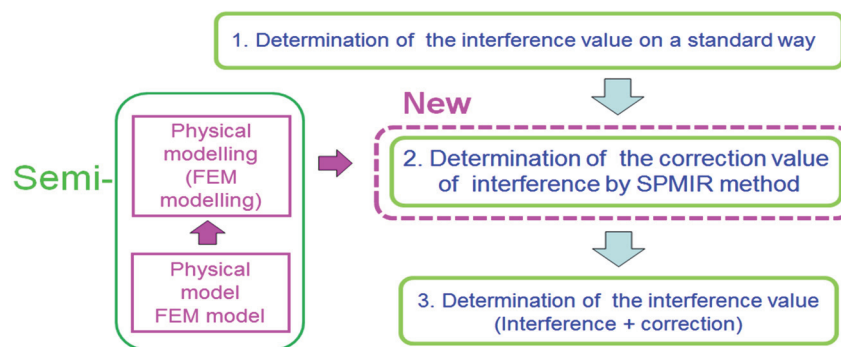


Fig. 4. The flow of design of pre-stressed micro-die.



realise that this asperity - because of its shape - provides the same Abbot-Firestone curve as the examined surface. It means that it is the statistical representation of all asperities. Further, it is than believed that “the reaction” for deformation under pressure of such a model is equal to the reaction of a “real” surface consisting of different asperities. In two dimensional, 2d-FEM, model both sharp ends of outside profile asperity, are neglected, figure 5 d. This model has arbitrary taken high H that has no influence on results. The roughness of the ring is assumed to be similar to the roughness of the die. Four FEM, models in 2d-plane strain conditions with a thickness b were created. During simulations, models of representative asperities were pressed with rigid planes to find four force revolutions $F_i(x)$ ($i=1,2,3,4$) and on the base of these four revolutions the mean contact pressure $q_i(x)$ (4) may be found for four following cases:

4. rough ring and ideal smooth and rigid die, figure 6d.

Simulations were conducted by MS Mark-Mentat 2015 package in static 2d-plane strain conditions with the material description as isotropic, elasto-plastic with strain hardening. Curves $q_i(x)$ are presented in figure 7.

$$q_i(x) = \frac{F_i(x)}{A}, i = 1,2,3,4 \quad (6)$$

where: $A = R_s \cdot b$

Curve 5 and 6 are functions $q_5(x)$ and $q_6(x)$ that meet the conditions (7) and (8) and might be respectively called: *Surface stiffness curve* of the die and *Surface stiffness curve* of the ring.

$$q_5^{-1}(x) = q_3^{-1}(x) - q_1^{-1}(x) \quad (7)$$

$$q_6^{-1}(x) = q_4^{-1}(x) - q_2^{-1}(x) \quad (8)$$

where: $q_5(x)$ – Surface stiffness curve of the die and $q_6(x)$ – Surface stiffness curve of the ring.

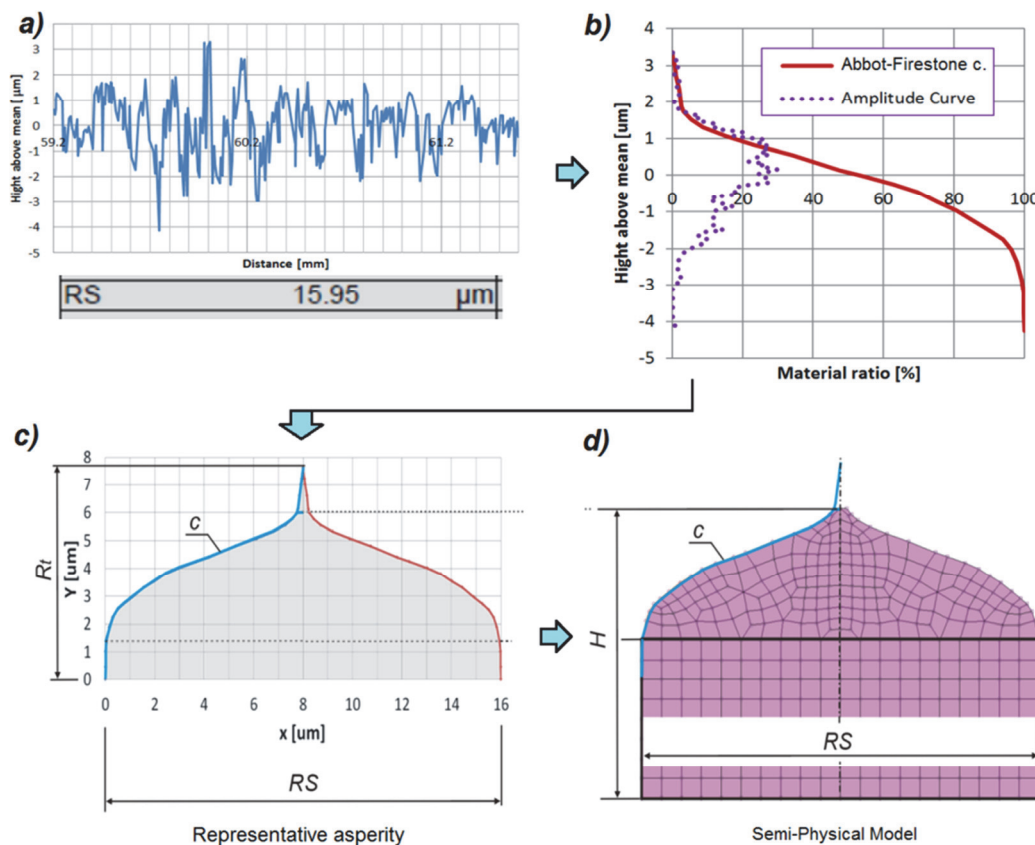


Fig. 5. Steps of creation Semi-Physical Model of surface roughness.

1. ideal smooth die and ideal smooth and rigid ring, figure 6a,
2. ideal smooth ring and ideal smooth and rigid die, figure 6b,
3. rough die and ideal smooth and rigid ring, figure 6c,

They represent revolution of mean contact pressure created only on the base of deformations of asperities, since deflection of core, curves 1 and 2, is subtracted (7), (8). For an assembling pressure of q , deflection of asperities might be calculated directly from figure 7. For die is equal to A and for ring is equal to B .



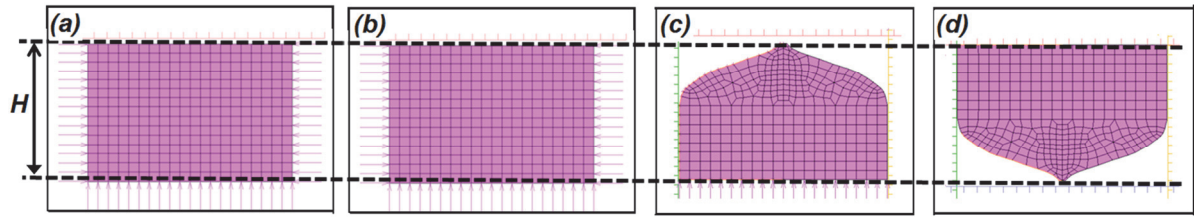


Fig. 6. FEM models: (a) ideal smooth die - limited movement of side and bottom nodes and smooth and rigid ring – rigid line, (b) ideal smooth ring - limited movement of the side and bottom nodes and smooth and rigid die – rigid line, (c) rough die - limited movement of bottom nodes and side rigid lines, smooth and rigid ring – rigid line, (d) rough ring - limited movement of bottom nodes and side rigid lines, smooth and rigid die – rigid line.

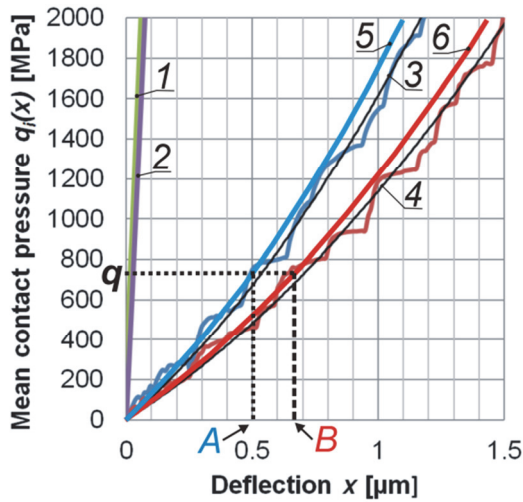


Fig. 7. Results of FEM: $q_i(x)$ where 1- smooth die, 2- smooth ring, 3 - rough die, 4 - rough ring, 5 and 6 described in text.

Would it that mean that *Contact surface stiffness curve* might be created by adding deflections A and B at each assembling pressure q?

The answer is: NOT. Because of at least two circumstances are not taken into account:

1. mutual influences of asperities of die and ring,
2. different relative positions of asperities of die and ring.

These weaknesses might be overtaken by the following method.

Let assume that exist $n+1$ relative positions of die and ring asperities, figure 8, that are described by the parameter e , see (9).

$$e_i = \frac{RS}{2 \cdot n} \cdot i, i = 0, 1, \dots, n \quad (9)$$

Than $n+1$ FEM – Marc Mentat 2015 - simulation are conducted for each of the relative positions of asperities – e_i . Here is the main point of the method. It is suggested that the limited set of $n+1$ mutual positions of representative single asperities represent the initial “situation” at the contact zone between rough “real” surfaces. The behaviour of such a contact might be fined on the base of results of $n+1$

“experiments” on $n+1$ “physical models” created with the help of FEM modelling. In FEM modelling the friction coefficient is stated as $\mu=0.3$. This value is chosen as a type of a compromise between sticking friction and no contact. The whole spectrum of “contact situations” is represented under the assembling pressure, figure 10. Each model consists of 4 deformable bodies: 1,2,3,4, figure 9a. The goal is to find a mean pressure evolution on the area of the representative asperity. Body 1 is separated by boundary conditions - no lateral movement of both side nodes. Bodies 2 and 3 are added on both sides of 1, since they have an influence on its deformation by the side deformations of body 4. Lateral movement of the left side nodes of 2 is also eliminated. Both sides nodes of 3 also can’t move laterally. The “wal” 8 additionally limits its deformation. Bottom nodes of 4 are fixed and both side nodes can’t move laterally. There are additionally two side “walls”

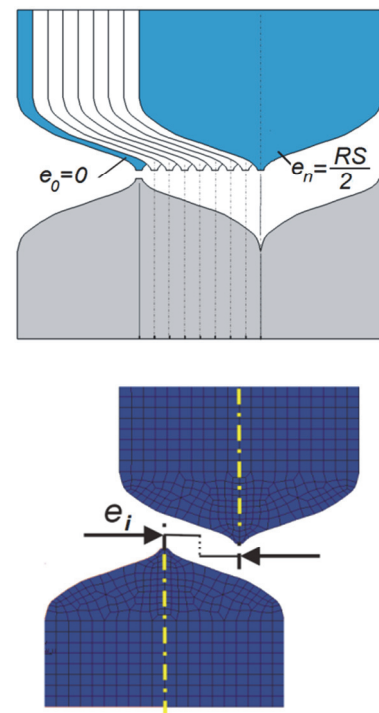


Fig. 8. Relative positions of die and ring asperities defined with parameter e .



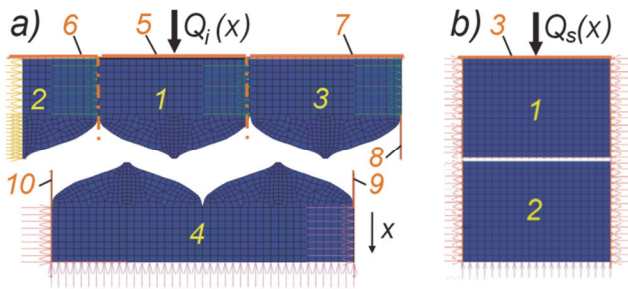


Fig. 9. FEM models of die-ring contact. (a) Model for $e=5$. (b) Model for ideal smooth die and ring.

9 and 10. During the simulation three rigid bodies: 5, 6 and 7 move down together along x axis.

Evolution of the force acting on 1 is recorded to let to obtain the evolution of the mean contact pressure $Q_i(x)$ for the i position. Additionally FEM analysis for smooth bodies, figure 9b must be conducted that let to obtain $Q_s(x)$ function.

It is proposed that the mean pressure revolution function $a(x)$ that is a contact stiffness of models might be obtained as arithmetical mean value of contact stiffness, $Q_i(x)$ for all $n+1$ cases, (10).

$$a(x) = \frac{1}{n+1} \sum_{i=0}^n Q_i(x) \quad (10)$$

where: $a(x)$ – contact stiffness of model, n – number of segment

Figure 10 shows visualization of behaviour of a pair of rough models of die and ring under different contact pressure. The linear distribution of relative positions of asperities of die and ring is being assumed.

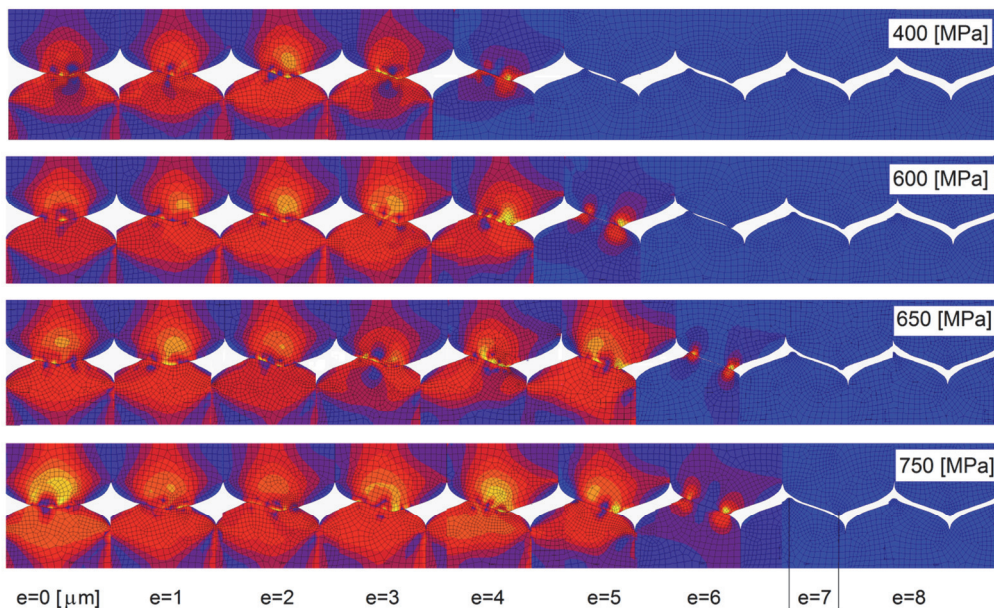


Fig. 10. Visualization of the behaviour of a pair of rough models of die and ring under different mean contact pressure, equivalent von Mises stress distribution.

Function $a(x)$, (8) express a contact stiffness of model – pair of rough bodies. To obtain a contact surface stiffness $c(x)$ one must take a contact stiffness of a pair of perfectly smooth bodies $Q_s(x)$ into account. Finally, the contact surface stiffness is a function that satisfies the equation (11).

$$c^{-1}(x) = a^{-1}(x) - Q_s^{-1}(x) \quad (11)$$

Function $c(x)$ is shown in figure 11. It let to directly find the radial interference correction ΔN_r for a certain assembling pressure p , dotted lines.

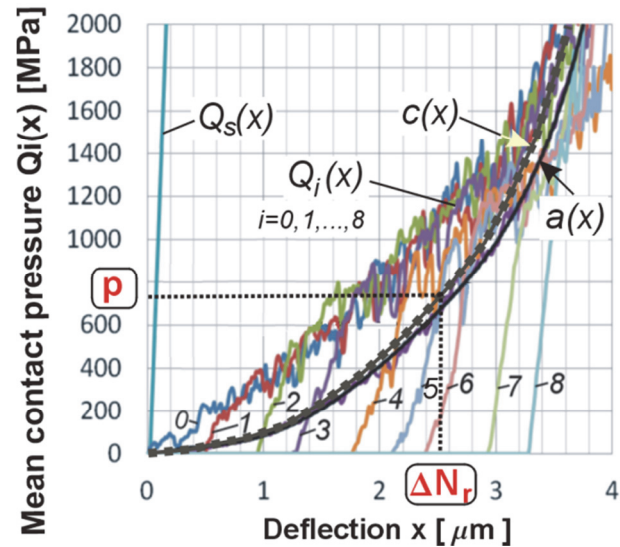


Fig. 11. Stiffness functions obtained on the base of FEM simulations results for 9 relative positions of representative roughness asperities of die and ring.



The correction of diameter interference as a function of assembling pressure, $\Delta N_m(p)$, might be also presented, figure 12. This graph is the final result of application of SPMIR method for pre-stressed micro-die design. It let to find (dotted line) for the applied assembling pressure $p=740$ MPa interference correction $\Delta N_m = 0.0052$ mm. Finally the corrected interference N_{m-cor} for this micro die follows the equation (12).

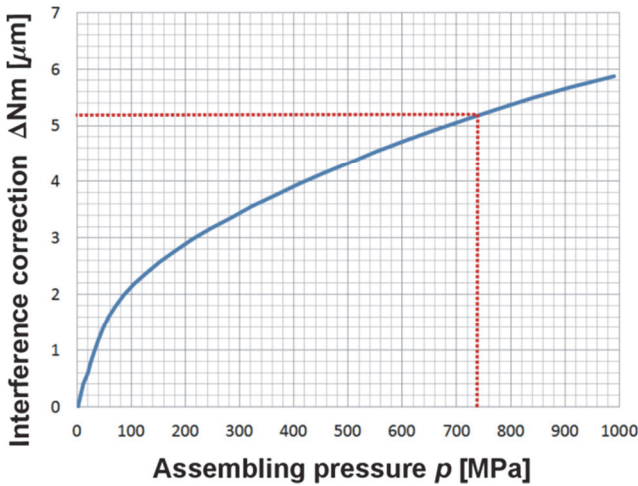


Fig. 12. Interference correction graph. The dotted line shows the interference correction for assembling pressure 740 MPa.

$$N_{m-cor} = N_m + \Delta N_m = 0.02034 + 0.0052 = 0.02554 \text{ [mm]} \quad (12)$$

The corrected value of initial assembling height is $h_{Ncor}=1.963$ mm, see (1), (2). Relative correction of diameter interference (13) exceeds 25%.

$$\Delta N_{m-rel} = \frac{\Delta N_m}{N_m} \cdot 100\% = 25.6\% \quad (13)$$

Such a big correction shouldn't be neglected.

4. THE SCALE EFFECT IN PRE-STRESSED MICRO-DIE DESIGN

The *scale effect* or *size effect* is a consequence of similarity theory (Xu et al., 2011) and was recognised on the field of metal forming with the development of microforming (Geiger et al., 1997). In general, two such effects are reported which are related to two phenomena: grain size (Justinger & Hirt, 2007; Shuaib et al., 2007) and behaviour of workpiece surface layer that affect friction (Tiesler, 2002). Concerning interference value of pre-stressed micro-dies the scale effect has been also observed. It might be called: *Pre-stressed micro-die assembling scale effect*.

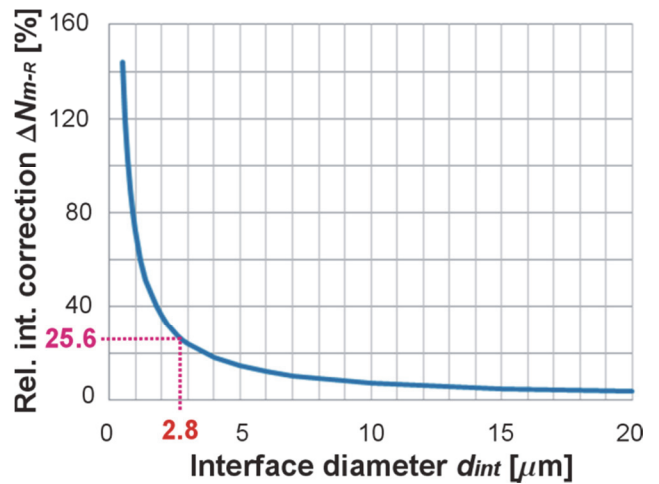


Fig. 13. Relative interference correction vs interface diameter. The worked case is marked.

Interference value depends on the interface diameter d_{int} . On another hand the proposed interference correction depends on contact pressure and Abbot-Firestone curves of the surfaces being in contact. The “shape” of these curves express surface manufacturing technology – for example: grinding. It means that for the fix manufacturing method the relative interference correction will increase with decreasing interface diameter. Figure 13 shows this tendency for analysed interface surfaces. The worked example of micro-die is there marked with the dotted line. Relative interference correction, figure 13, is hyperbolically increasing with decreasing interface diameter, exceeding 10 % for interface diameter about 8 mm. Further, at 3 mm is about 25 % but at 2 mm almost 40%.

5. CONCLUSIONS

- The new SPNIR method of determining the die insert diameter correction for pre-stressed micro-dies was proposed. It uses *contact surface stiffness curve* which is determined on results of a set of FEM experiments on semi- physical models of interface roughness. Objects for FEM analysis are created on the base of Abbot-Firestone curves.
- Relative correction of die diameter interference increases with decreasing of this diameter that might be recognized as a *pre-stressed micro-die assembling scale effect*.
- Relative interference correction is hyperbolically increasing with decreasing interface diameter, exceeding 10 % for diameter about 8 mm. Further, at 3 mm is about 25 % but at 2 mm almost 40%. It is strongly advised to use correction of



determined interference for dies with interface diameter less than 10 mm.

- Interference correction based on roughness profile of the interface surface might be skipped for pre-stressed dies with interface diameter bigger than 20 mm. The relative interference correction is about 3.5 % at this point and decreases with diameter increase.

ACKNOWLEDGEMENTS

The work reported in this paper is financially supported by the National Science Centre, Poland (UMO-2011/01/B/ST8/07731)

REFERENCES

- Geiger M., 2001, Microforming, *CIRP Annals – Manufacturing Technology*, 50 (2), 445-462.
- Geiger M., Messner A., Engel U., 1997, Production of micro-parts – Size effects in bulk metal forming, similarity theory, *Production Engineering*, 4, 55-58.
- Justinger H., Hirt G., 2007, Analysis of size-effects in the miniaturized deep drawing process, *Key Engineering Materials, Sheet Metal*, 344, 791-798.
- Lange K., 1985, *Handbook of Metal Forming*, McGraw-Hill Book Company.
- Lipa Z., Tomanickova D., 2011, Utilization of Abbot-Firestone Curves Characteristics for the Determination of Turned Surface Properties, *Annals of Faculty Hunedoara - Int. Journal of Eng.*, IX(3), 223-226.
- Presz W, Rosochowski A., 2006, The influence of grain size on surface quality of microformed components, *The 9th Int. Conf. on Material Forming, ESAFORM 2006*, Glasgow UK, Krakow, Publishing House Acapit, 587-590.
- Presz W., 2009, The Influence of Side Flats on Stresses in a Thick Tube, *FiMM-2009, Oficyna Wyd.PW. Prace naukowe, Mechanika*, 226, 137-142.
- Shuaib N., Khraisheh M., Rawashdeh O., 2007, Size effects on strain limits of thin CuZn30 brass sheets, *Proceedings of the 2nd International Conference on Micro Manufacturing (ICOMM)* Clemson University, Clemson SC, 140-144.
- Sieber. K., 1971, Theoretical Principled and Practical Experience for the Design of Cold Extrusion Tools, *Metal Forming*, 101-105, 128-131.
- Tiesler N., 2002, Microforming - Size effects in friction and their influence on extrusion processes, *Wire*, 52, 1, 34-38.
- Xu J., Guo B., Shan D., 2011, Size effects in micro blanking of metal foil with miniaturization, *Int J Adv Manuf Technol*, 56, 5-8, 515-511.

EFEKT SKALI W PROJEKTOWANIU WSTĘPNIE SPRĘŻONYCH MIKRO-MATRYC DO MIKRO-OBROBKI PLASTYCZNEJ

Streszczenie

W matrycach do wyciskania na zimno dopuszczalne ciśnienie wewnętrzne może być podwyższone poprzez użycie jednego lub dwóch pierścieni sprężających. Taka konstrukcja powoduje powstawanie wstępnych naprężeń rozciągających w pierścieniu/pierścieniach, a ściskających w matrycy. Projektowanie, w zasadzie, sprowadza się do określenia wielkości wcisku jaki ma być osiągnięty podczas montażu. Wcisk determinuje właściwości matrycy i musi być precyzyjnie określony. W zasadzie, stosuje się dwie metody projektowania: analityczną opartą na rozwiązaniu Lamé oraz MES. Żadna z tych metod nie uwzględnia chropowatości powierzchni kontaktu matrycy i pierścienia. Przykład wstępnie sprężonej mikro-matrycy pokazuje, że chropowatość kontaktu nie może być pomijana i wielkość wcisku uzyskana metodami „klasycznymi” wymaga korekty. Zaproponowano nową metodę określania tej wielkości: metodę SPMIR. W tej metodzie prowadzonych jest szereg symulacji MES z wykorzystaniem modeli kontaktu zbudowanych na podstawie krzywych Abbota-Firestone określonych z profilu chropowatości. Symulacje prowadzą do określenia krzywej sztywności kontaktu matryca-pierścień i w konsekwencji do określenia wielkości poprawki wcisku. Względna poprawka wcisku rośnie wraz ze zmniejszaniem się średnicy kontaktu, co można uznać za efekt skali w odniesieniu do projektowania wstępnie sprężonych mikro-matryc. W analizowanym przykładzie, względna korekta wcisku rośnie hiperbolicznie wraz ze spadkiem średnicy kontaktu. Przekracza ona 10% w wypadku średnicy około 8 mm, 25% przy średnicy 3 mm i prawie 40% przy średnicy 2 mm. Proponowana metoda jest zalecana przy projektowaniu mikro-matryc o średnicy kontaktu matrycy z pierścieniem poniżej 8 mm.

Received: November 09, 2016

Received in a revised form: March 21, 2017

Accepted: April 04, 2017

